SUPPORTING INFORMATION

Three-phase reversible mechanochemical interconversion of hydrogen-bonded melamine:barbiturate co-crystals: from rosette to linear tape polymorphs

Inês C. B. Martins,*[a+] Ana M. Belenguer,*[b+] Giulio I. Lampronti,[c] and Petr Motloch*[b]

Contents

1 Experimental Section: Materials and Equipment

1.1 Materials

The chemicals for the synthetic procedure were obtained from commercial suppliers and used without further purifications unless stated otherwise. 4-tert-butylaniline (CAS [769-92-6] from Acros Organics), cyanuric chloride (CAS [108-77-0] from Thermo Scientific), N,N'-di-isopropyl ethylamine (CAS[7087-62-5] from Acros Organics) , $MgSO_4$ (Fisher, lab reagent grade).

Solvents used in the synthetic procedure were either distilled before use or used as obtained. Tetrahydrofuran (THF), ethyl acetate (EtOAc) and petroleum ether (PE) 40-60^oC were distilled in house, 1,4-dioxane (Fisher, lab reagent grade), NH_4OH.

All solvents used for ball milling experiments were obtained as follows: acetonitrile (MeCN), methanol (MeOH), isopropanol (IPA), toluene and water were HPLC grade from Fisher Scientific.

1.2 Equipment and methodology used for the preparation procedure

For purification of the prepared compounds, automatic chromatography systems CombiFlash R_f^+ and CombiFlash R_f^+ Lumen (with UV light detection at 254 nm and 280 nm and evaporative light scattering detector for Lumen) with pre-packed puriFlash columns from Interchim (silica, 25 µm) and with a sample loading of mixtures on Celite, were used.

The microwave used was Biotage Initiator$^+$.

The melting point was recorder on a Mettler-Toledo MP90 system.

^{1}H NMR spectrum was recorded on Bruker 400 MHz Avance III HD SmartProbe Spectrometers at 400 MHz. All chemical shifts are quoted in ppm and were referenced to the residual peaks of used solvent: CD_3OD (^{1}H: 3.31 ppm). Coupling constants *J* are stated in Hz.

The reactions were monitored by LCMS Waters Acquity H-class UPLC system coupled to a single quadrupole Waters SQD2

1.3 Ball milling equipment

1.3.1 Ball mill grinder

The ball milling experiments were all performed using a Retsch MM400 Shaker Mill with a fixed amplitude of 20 mm, a variable frequency of 3-30 Hz and a timer up to 99 minutes. The manufacture's safety cover was removed as the grinder motor vents to the front of the equipment warming the milling jars on prolonged milling. An external safety shield was used for safety as shown in Figure S1.

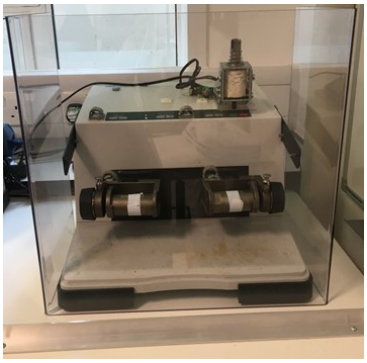

Figure S1. Modified Retsch MM400 Shaker Mill (ball mill) with a solenoid installed to remotely press the START button and with the manufacturer's safety cover removed and replaced by an external safety shield.

1.3.2 Milling jars

The milling jars were manufactured in-house from AISI440C stainless steel with a 14.5 mL internal volume, 19 mm internal diameter x 52 mm internal length, the closure being a screw closure lined with a Teflon washer to ensure good sealing when the milling jar is closed. The clean machined jars were subjected to a hardening and tempering process to reach + 56HRC (Rockwell Hardness Scale C). The hardening and tempering process of the AISI440C stainless steel screw closure jars was performed by WALLWORK CAMBRIDGE LTD. This design should prevent the escape of the vapor phase of the solvent. It should also prevent powder and added solvent from being trapped in the junction of the closure while avoiding damage to the thread of the screw closure. See Figure S2-a). All the ball bearings were sourced from Dejay Distribution Ltd.

a) b) c)

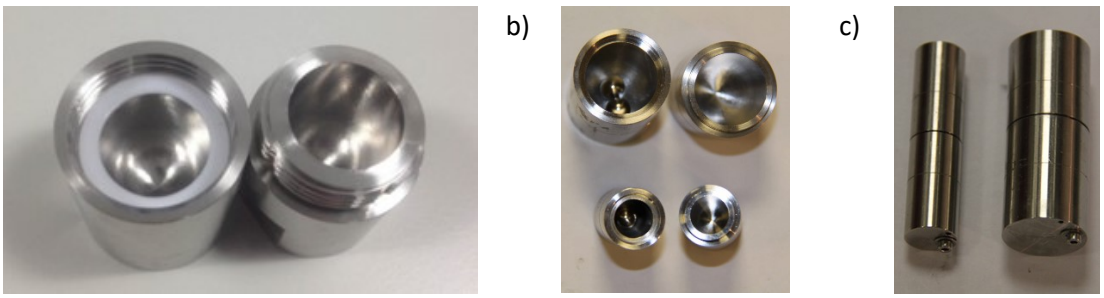

Figure S2. a) 14.5mL (19 mm internal diameter x 52 mm internal length) homemade screw closure milling jars made from 440C stainless steel jars with Teflon washer. b) bottom and c) left side, 4 mL narrow homemade snap closure millling jar / (10 mm internal diameter x 56 mm internal length) made from 316 stainless steel jars. (b) top and c) right side displays the wider 19 mm internal diameter snap closure jar, which is shown here for comparison.

1.3.3 Milling jar heating mantel

The custom-made heating mantle used to heat the milling jars was obtained from Holroyd Components Ltd. The heating mantle was designed to wrap round the cylindric milling jar, had a dimension of 25x55mm, with 20W and 12V potential. The controller for the heating mantel was designed and manufactured in house.

1.4 PXRD equipment

1.4.1 Powder X-ray diffractometer

X-ray powder diffractograms in the 2θ range 4-45° (Cu Kα radiation, step size 0.03°, time/step 100 s, 0.04 rad soller, VxA 40x40) were collected either (1) on an X-Pert PRO MPD powder X-ray diffractometer or (2) on a Panalytical X'Pert Pro diffractometer both equipped with an X'Celerator detector. Both PXRD equipment were available at the Department of Chemistry, University of Cambridge.

1.4.2 PXRD sample preparation holders

Glass PXRD sample slides (10 x15 mm) with the 2 mm rectangular recess were used with the X-Pert PRO MPD powder X-ray diffractometer.

Circular glass slides with a depression were installed in a holder with a clamp when the Panalytical X'Pert Pro diffractometer was used in the spinning mode.

2 Solution based experimental procedures

2.1 Synthesis of ME

The synthesis of 2,4-bis(4-(tert-butyl)phenyl)-1,3,5-triazine-2,4,6-triamine (**ME**) was performed according to the published procedure.[1] Briefly, 4-tert-butylaniline (2 mL, 14.3 mmol) was added to a solution of cyanuric chloride (1.2 g, 6.5 mmol) and di-isopropyl ethylamine (5 mL) in THF (100 mL) and left stirring overnight. Then, the solvents were removed under reduced pressure. The residue was portioned between EtOAc (130 mL) and brine (75 mL). The organic phase was washed with additional brine (70 mL) and dried over $MgSO_4$ and the solvent was removed under reduced pressure. The crude was transferred into a microwave vial. 1,4-dioxane (5 mL) and NH_4OH (15 mL) were added, and the vial was capped. The mixture was heated for 15.5 hours at 95 °C inside of a microwave. After cooling, the solvents were removed under reduced pressure. The residue was portioned between EtOAc (150 mL) and brine (100 mL). The organic phase was washed with additional brine (50 mL) and dried over $MgSO_4$. The solvent was then removed under reduced pressure. A combiflash of the residue on silica (80 g, solid loading, Petroleum Ether (PE) and EtOAc, PE: EtOAc 0%→100%) provided the title compound (1.4 g, 55% yield) as a white solid.

2.2 Characterisation of ME

^{1}H NMR ($CDCl_3$/CD_3OD, 400 MHz, 298 K): δ 7.41 (d, J = 8.5 Hz, 4H), 7.29 (d, J = 8.5 Hz, 4H), 1.28 (s, 18H). (referenced to CD_3OD)

MP: 287 – 289 °C

MS: (ESI): 391 $[M+H]^+$

The data was in agreement with the previously published data.[1]

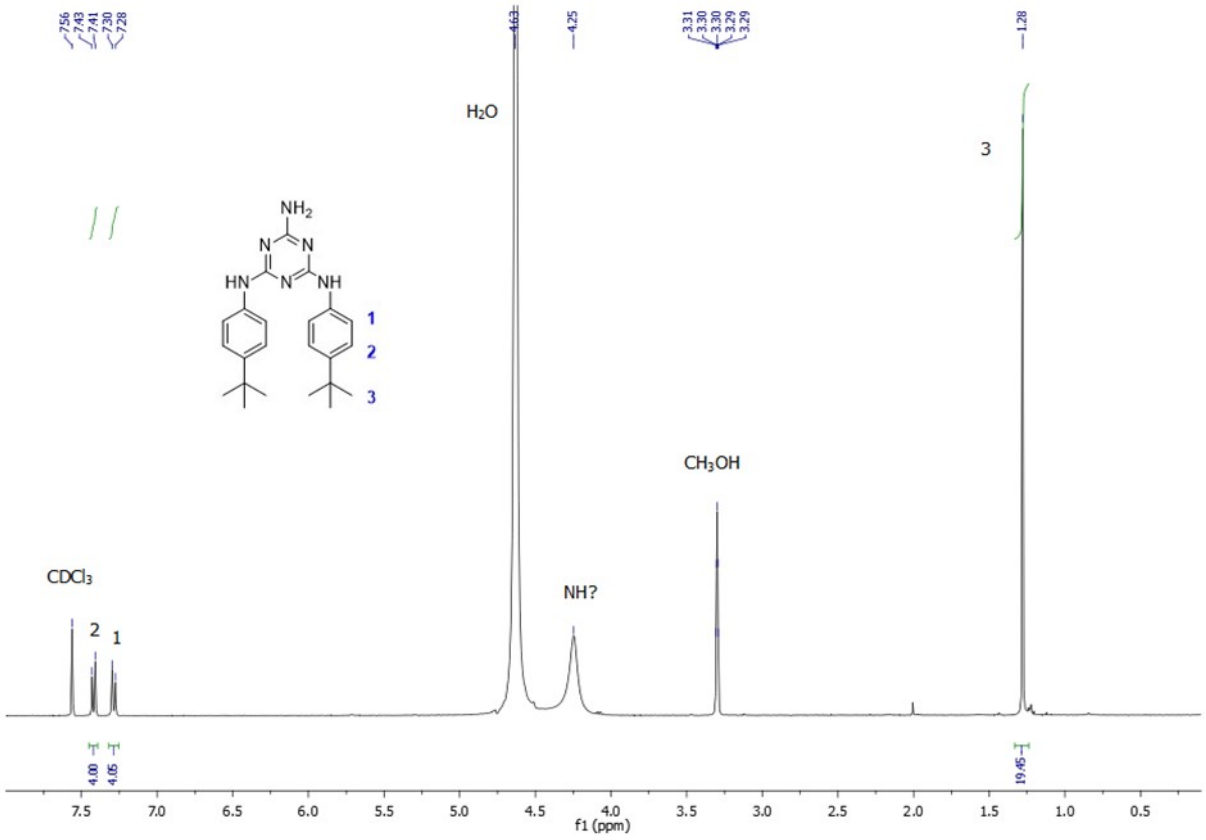

Figure S3. ^{1}H NMR spectra of **ME**.

LCMS conditions: UPLC Column (Acquity Premier Protein BEH C4 300A 1.7 um, 2.1 x 50 mm).

Solvent A: Water + 0.1% formic acid;
Solvent B: Acetonitrile + 0.1% formic acid;
Gradient: 0 – 2 minutes 5% – 100%B + 1 minute 100%B);
flow rate (0.6 ml/min); column temperature of 40 °C.

The UV signal was monitored at 254 nm (See chromatogram in Figure S5-a) and 280 nm, and in (+)-ESI in MS (See MS trace in in Figure S4-b).

a)

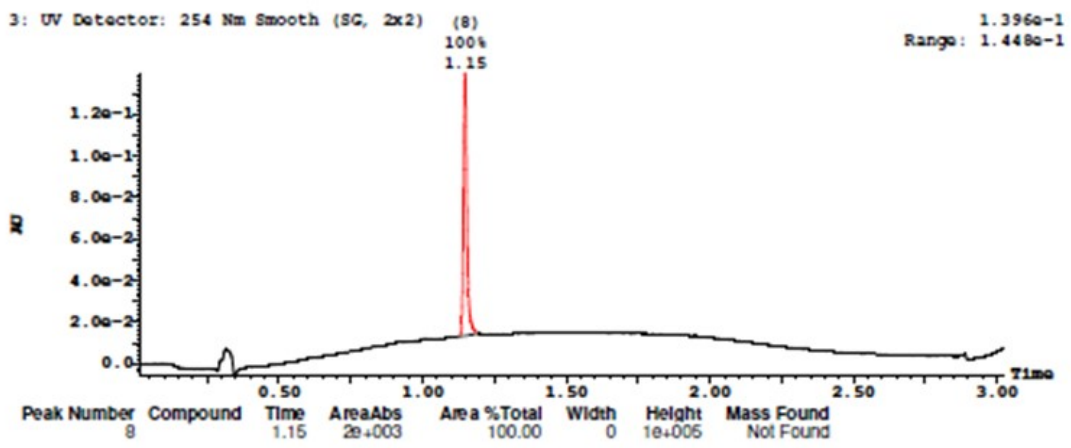

b)

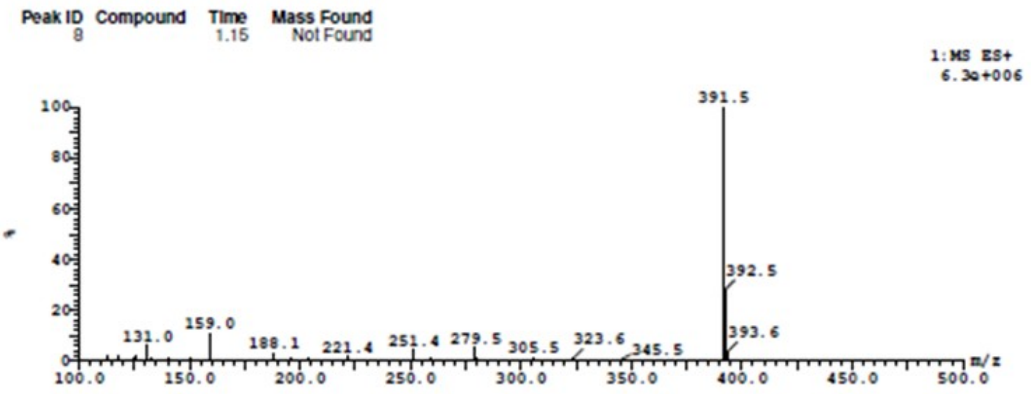

Figure S4. LCMS by electrospray ((+)-ESI) of **ME**. a) UV chromatogram monitored at 254 nm. b) (+)-ESI MS at 1.15 min where ME elutes under the LCMS conditions used.

3 General background on polymorph formation and interconversion by ball milling

Ball milling is an innovative, clean, effective, and highly atom-efficient approach to the solid-state synthesis of molecules and preparation of co-crystals. Depending on the milling conditions, different polymorphs can be obtained. Ball mill neat grinding or NG is when milling is performed in the absence of added liquid. Ball mill liquid assisted grinding or LAG is when milling is performed in the presence of added liquid.

The kinetic profile of a ball mill reaction is characterised by 3 stages as illustrated in Figure S5. First, the induction stage where the starting materials or co-formers are being comminuted in preparation to react with each other. This stage can sometimes be very short, a matter of seconds or just a minute, or very long (sometimes hours) before the reactants start reacting. Next, comes the reaction stage, moving at the end to the steady-state stage. For some systems, the reaction stage could be instantaneous,

taking much less than one minute to reach a steady-state. For other systems, the reaction stage is slow to reach a steady-state. At steady-state, the reaction is complete: further milling will not alter the phase composition as illustrated in Figure S5. To obtain the final product or the desired co-crystal at maximum yield, it is important to reach a steady-state. The best strategy is to mill well in excess to what is absolutely needed to ensure we are at steady-state.

Figure S5 illustrates a typical kinetic profile of the mechanochemical formation of either a product from 2 equimolar starting materials or of a co-crystal from 2 equimolar co-formers. The kinetics are often slower under NG (Figure S5-a) than under LAG conditions (Figure S5-b). The example of Figure S5 shows that under NG conditions, only **Form I**, favored by these milling conditions, will be exclusively formed; the other potential polymorph (**Form II**) is not formed. Under LAG conditions, the formation of **Form II** is now favored and **Form I** is not formed. Often LAG transformation resulting in the formation of **Form II**, can happen with a variety of LAG solvents. However, each solvent requires a minimum threshold of added volume to achieve the formation of **Form II**, otherwise **Form I** will be formed. In some cases, the use of different LAG solvent types may favor the formation of a different polymorphs (*e.g.***Form III**). This milling behaviour is shown by most of the molecular reactions[2-7] or by the formation of co-crystals[8] we have investigated so far.

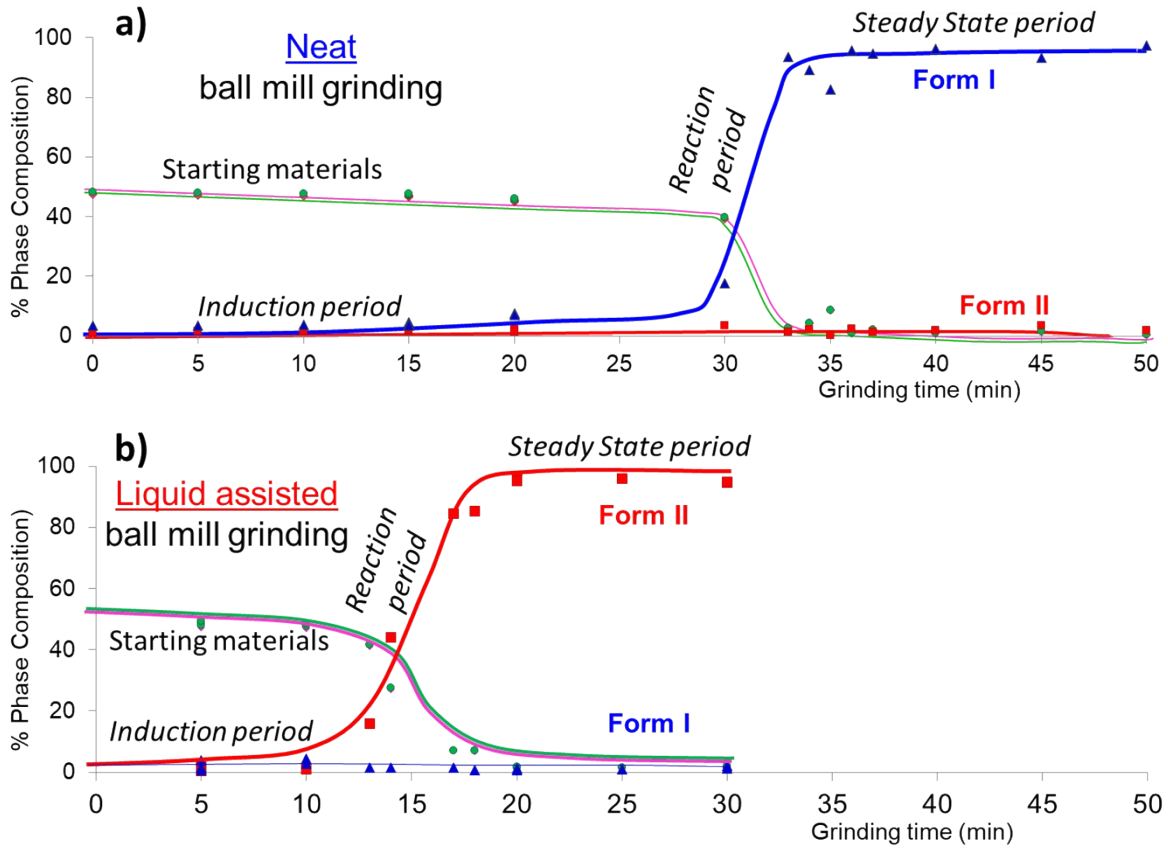

Figure S5. Typical kinetic profile of the mechanochemical reaction under a) NG and b) LAG conditions. The data is obtained by Rietveld refinement of the ex-situ PXRD patterns. The kinetic profile of all mechanochemical reactions have 3 phases: induction, reaction and steady-state. a) Under NG conditions, **Form I** is quantitatively formed, while **Form II** is absent. b) Under LAG conditions, **Form II** is quantitatively formed, while **Form I** is absent.

Polymorphs can interconvert by applying the milling conditions favoring a specific polymorph. In the example of Figure S5, NG to steady-state will always favor the formation of **Form I**; Therefore, under NG conditions, **Form II** will interconvert to **Form I**, if milling is performed for long enough to achieve

steady-state. Conversely, LAG will favor the formation of **Form II**. Therefore, under LAG conditions, **Form I** will interconvert to **Form II**, if milling is performed for long enough to achieve the steady-state.

4 Strategy to investigate polymorphs of 1:1 ME:BA obtained by ball milling.

4.1 Background and strategy

We used the knowledge gained from our experience in mechanochemistry (See Section 3) to investigate which polymorphs of the **1:1 ME:BA** co-crystal can be obtained by changing the experimental milling conditions.

We decided from the outset to use the 14.5 mL screw closure homemade jars (Figure S2-a), for method development as we had a lot of experience with this jar geometry. The loading in these jars is typically around 200-300 mg. For loadings below 100 mg we decided to use the narrower (4mL internal volume, 10 mm ID x 56 mm internal length) snap closure jar (Figure S2-b (bottom) and Figure S2-c (right))

It was clear from the beginning that the few grams of **ME** produced by the synthesis (See Section 2.1) was not sufficient for a full method development starting from the co-formers (**ME** and **BA**) each time. This was only a challenge, not a limitation.

From our previously published work on the fundamentals of ball milling, we were confident that all polymorphs of the **1:1 ME:BA** co-crystal should be able to interconvert. This would allow us to recycle the powder inside the jar many times and convert one polymorph to another by just applying the correct experimental milling conditions and milling to a steady-state. Therefore, most of the development work presented here uses recycled powder to investigate the required experimental conditions to obtain the different polymorphs. We investigated NG conditions to steady-state. LAG conditions were investigated using different solvent types and volumes, milling them to a steady-state. From our published work we knew that the same outcome should be obtained when milling with the right stoichiometry, starting from the co-formers or when starting from any intermediate or final product obtained with the right stoichiometry of the co-formers.

We named **Form A**, the published rosette polymorph,[1] as depicted in Figure S6.

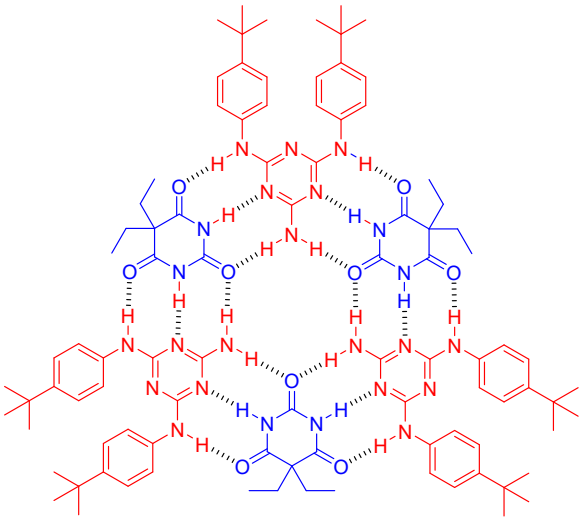

Figure S6. Chemical structure of the published Rosette polymorph of 1:1 **ME:BA** co-crystal,[1] named now **Form A**.

The calculated PXRD pattern for the published rosette polymorph **Form A** (Figure S7) was obtained from the CCDC database with the refcode KUFPIK.

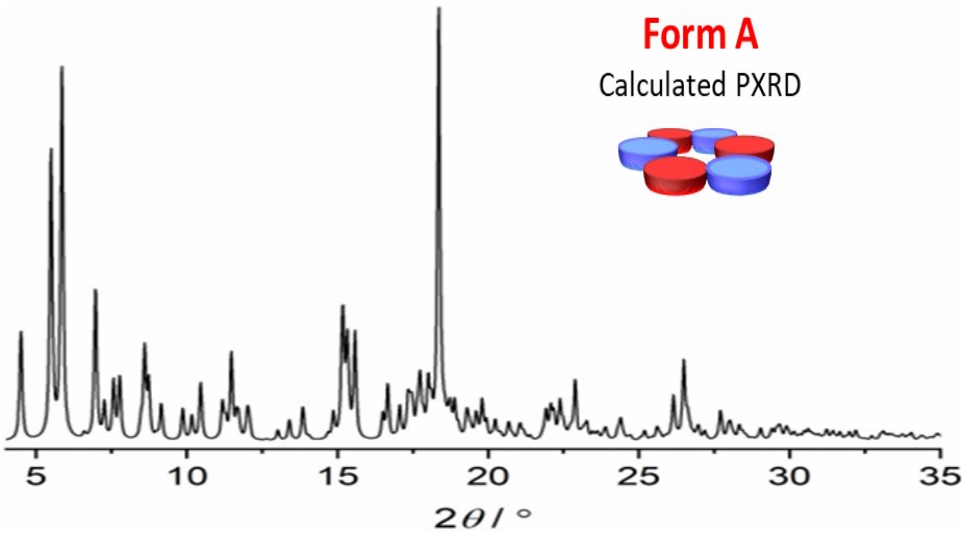

Figure S7. Calculated PXRD pattern of the published rosette polymorph **Form A**, obtained from CCDC (refcode KUFPIK).

4.1.1 Use of elevated temperatures on ball milling

As part of the method development, we heated the milling jar to check if the increase of temperature had an effect on the outcome. We could prove for the 1:1 **ME:BA** co-crystal that the product obtained by milling under elevated temperature was the same as that obtained at ambient temperature. This is consistent with Descamps and co-workers findings where the T_g with respect to the milling temperature is the key factor that determines the end product of the milling process. A T_g above the milling temperature typically forms an amorphous material.[9] Synchrotron monitoring while heating the milling jar demonstrated polymorph transformation of α-polymorph to β-polymorph of 1-adamantyl-1-diamantyl ether (ADE) at high temperature.[10] In a similar way, Emmerling *et al.* demonstrated on *in situ* synchrotron experiments that Form I of the NA:PA co-crystal transforms to Form II just around 65°C when heating the milling jar.[11]

4.2 Mechanochemical preparation of 1:1 ME:BA Form A. Procedure

Equimolar amounts of **ME** (0.52 mmol, 203.1 mg) and **BA** (0.52 mmol, 95.8 mg) were added to a 14.5mL home-made screw closure jar. The crystals of **ME** and **BA** were manually mixed in the jar with a microspatula. Two 7.0 mm 440C stainless steel balls were added to the jar. 50 µL of acetonitrile was dispensed on top of the powder, avoiding direct contact with the powder. The jar was screwed tightly and secured with insulating tape. After installing the jar in the MM400 ball mill, it was milled for 1 hour at 30 Hz obtaining quantitative **Form A** at steady-state.

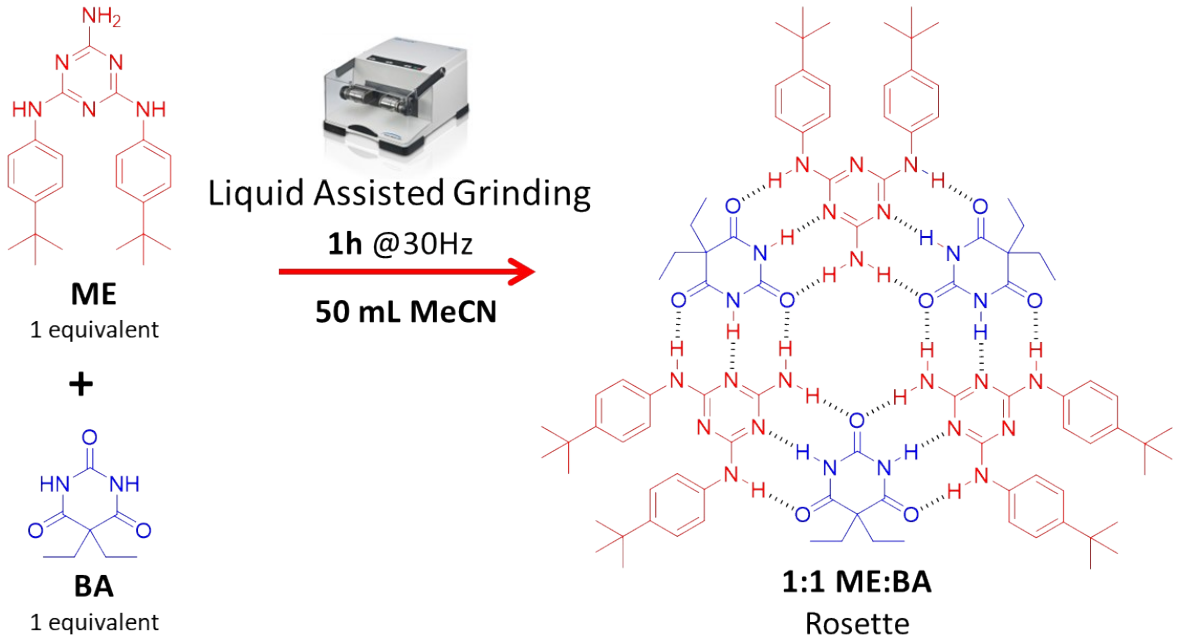

Figure S8. Chemical scheme of the mechanochemical preparation of **Form A** co-crystal (Rosette) of 1:1 **ME:BA**.

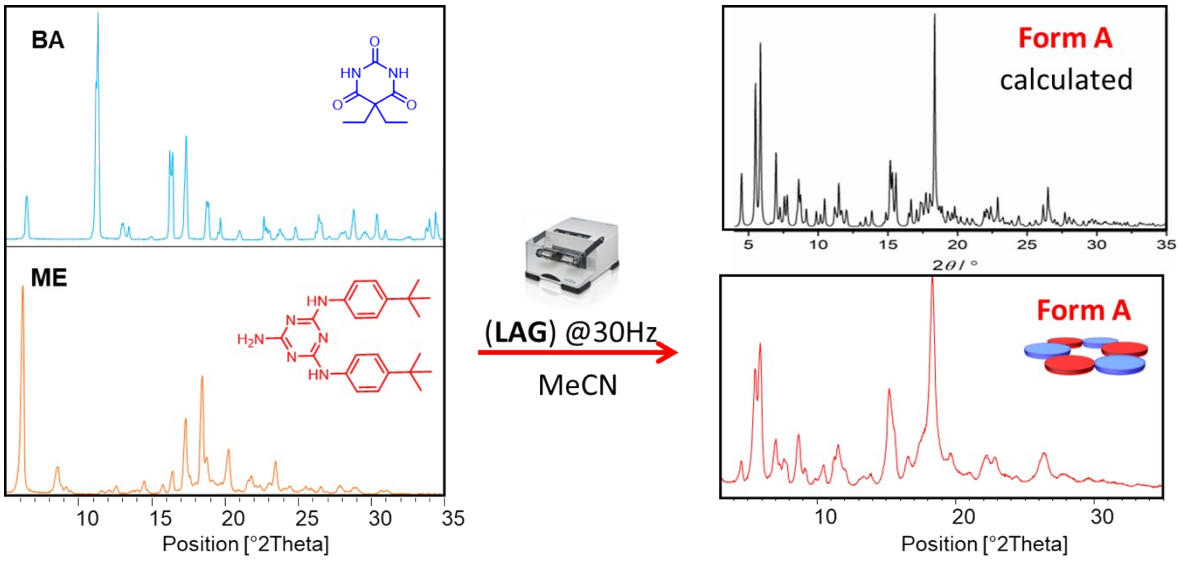

Figure S9. PXRD patterns of the mechanochemical preparation of **Form A** co-crystal (Rosette): On the left, the 2 co-formers (top left: **BA**) and (bottom left: **ME**). On the right is PXRD of the rosette co-crystal. Top right: calculated rosette polymorph and bottom right: **Form A** (rosette) obtained by ball mill LAG to a steady-state using MeCN.

4.3 Mechanochemical preparation of amorphous form. Procedure

Equimolar amounts of **ME** (0.52 mmol, 203.1 mg) and **BA** (0.52 mmol, 95.8 mg) were added to a 14.5 mL home-made screw closure jar. The crystals of **ME** and **BA** were manually mixed in the jar with a microspatula. Two 7.0 mm 440C stainless steel balls were added to the jar. The jar was closed and secured with insulating tape. On installing the jar in the MM400, it was milled under neat grinding conditions for 1 hour at 30 Hz reaching close to a steady-state. The resulting powder was found to be very static and amorphous. Some small peaks corresponding to residual barbital were obvious in the PXRD pattern shown in Figure S10.

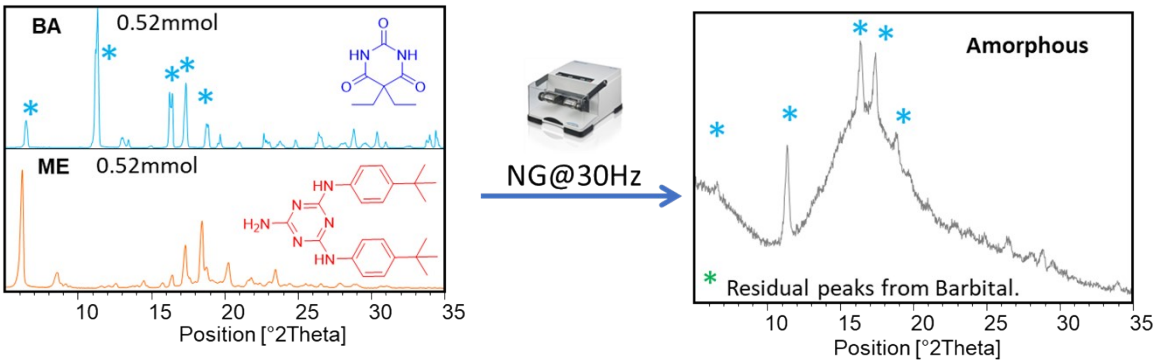

Figure S10. PXRD pattern of the 2 co-formers on the left (top left: **BA**) and (bottom left: **ME**) and on the right of the predominant **amorphous form** of 1:1 **ME:BA** co-crystal obtained by ball mill neat grinding (NG) to a steady-state. Residual **BA** (*) can be observed by comparing the peaks of the PXRD pattern of the predominant **amorphous form** with that of **BA**.

4.4 Mechanochemical synthesis of Form B

Form B has been obtained either starting from the **amorphous form** (Section 4.4.1 and Figure S11) or starting from **Form A** (Section 4.4.2 and Figure S12) by ball mill LAG at 30 Hz to a steady-state with 50 µL or 100 µL water. **Form B** has been never attempted to be obtained directly starting from equimolar amounts of **ME** and **BA**. (See Section 8).

4.4.1 Preparation of Form B starting from amorphous form: Procedure

Form B was obtained by adding 50 µL water over the synthesised powder of the **amorphous form** (298.8 mg) which was contained inside the 14.5 mL milling jar with two 7.0 mm balls. The synthesis of this **amorphous form**, to be now recycled, was previously described in Section 4.3. The PXRD patterns of co-formers and **amorphous form** are shown in Figure S10. The milling jar was then screwed tightly, installed in the MM400 ball mill, and milled for 1 hour at 30 Hz reaching steady-state and obtaining **Form B** quantitatively. The PXRD pattern of **Form B** is shown in Figure S11.

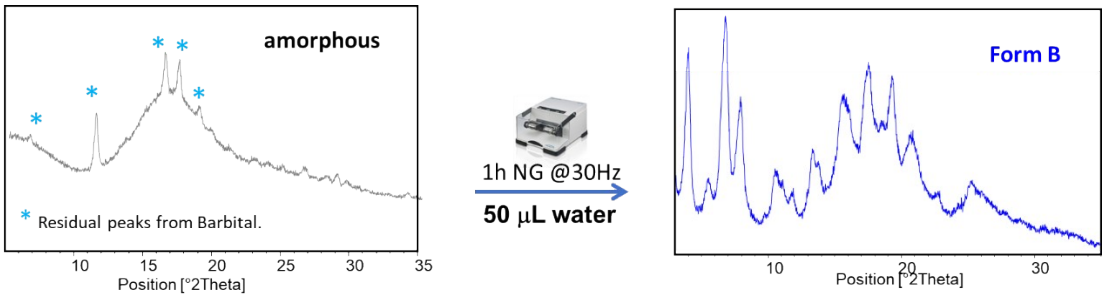

Figure S11. Preparation of **Form B** by ball mill LAG with 50 µL water starting from the **amorphous form**.

4.4.2 Preparation of Form B starting from Form A: Procedure

Form B was obtained by adding 100 µL water to in-situ dried powder of **Form A** (298.8mg) contained in the 14.5 mL milling jar with two 7.0 mm balls. The preparation of this **Form A**, to be now recycled, was previously described in Section 4.2 and PXRD pattern shown in Figure S9. This jar was screw closed, installed in the MM400 ball mill and milled for 2h at 30 Hz, reaching a steady-state and obtaining **Form B** quantitatively. The PXRD pattern of **Form B** is shown in Figure S12. In hindsight, heating the powder at 40°C is not believed to be required for the polymorphic transformation but heating can improve the rate of transformation (See 4.1.1).

Figure S13-f indicates that the transformation of **Form A** to **Form B** is also achieved by LAG to a steady-state with just 50 µL water.

Figure S12. Preparation of **Form B** by ball mill LAG with water starting from **Form A** (rosette).

5 Milling conditions required for polymorph interconversion between Form A, Form B and the amorphous form

In Section 4.4 we have presented the procedure to synthesise **Form B** starting from **Form A** or from the **amorphous form** by polymorph interconversion.

We will now discuss the required milling conditions to transform the following:

Section 5.1: **Amorphous form** to **Form B**
Section 5.2: **Form A** to **Form B**
Section 5.3: **Form B** to **Form A**
Section 5.4: **Form B** to **amorphous form**
Section 5.5: **Form A** to **amorphous form**
Section 5.6: **Amorphous form** to **Form A**

5.1 Milling conditions to transform the amorphous form to Form B

As described in Section 4.4.1, LAG with water milled to steady-state will result in the quantitative formation of **Form B** as shown in Figure S11, discussed previously.

5.2 Milling conditions to transform Form A to Form B

The following exploratory experiments demonstrate that **Form A** is only transformed to **Form B** by ball mill LAG with water (Figure S13-f). This happens only with extended milling so that a steady-state is reached. The attempts to mill **Form A** by LAG in the presence of toluene, n-heptane and IPA did not result in any polymorph transformation. While we milled during exploratory experiments at 40°C for LAG with water, we believe from previous experience that milling under ambient temperature would not have changed the outcome significantly (See 4.1.1), though this transformation on Figure 13-f may have displayed even slower kinetics. Figure S12 also show a full polymorph transformation from **Form A** to **Form B** by LAG with 100 µL water. So, excess of water works well too.

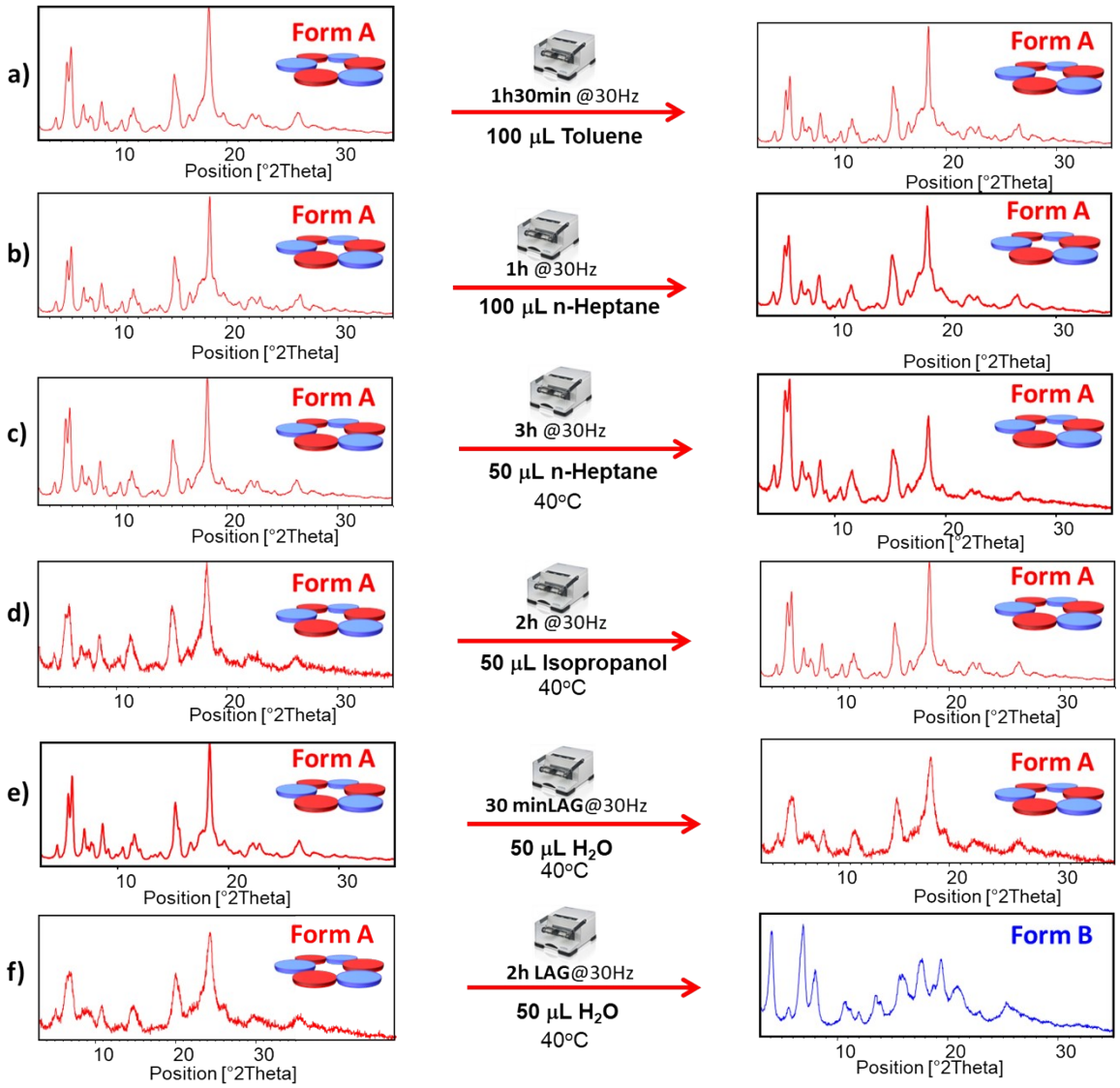

Figure S13. Exploratory milling experiments by LAG with different solvents (a) toluene. b) & c) n-heptane, d) IPA and e) & f) water, to interconvert **Form A** (rosette) to **Form B**. Only LAG with water for extended milling time (2h) achieved a steady-state, transforming **Form A** to quantitative **Form B**.

5.3 Milling conditions to transform Form B to Form A

It has been found that **Form B** can be transformed to **Form A** by LAG with at least 3 different solvents: MeCN (Figure 14-a), ethyl acetate (Figure 14-b) and methanol (Figure 14-c). The milling temperature may only affect the rate of transformation (See 4.1.1).

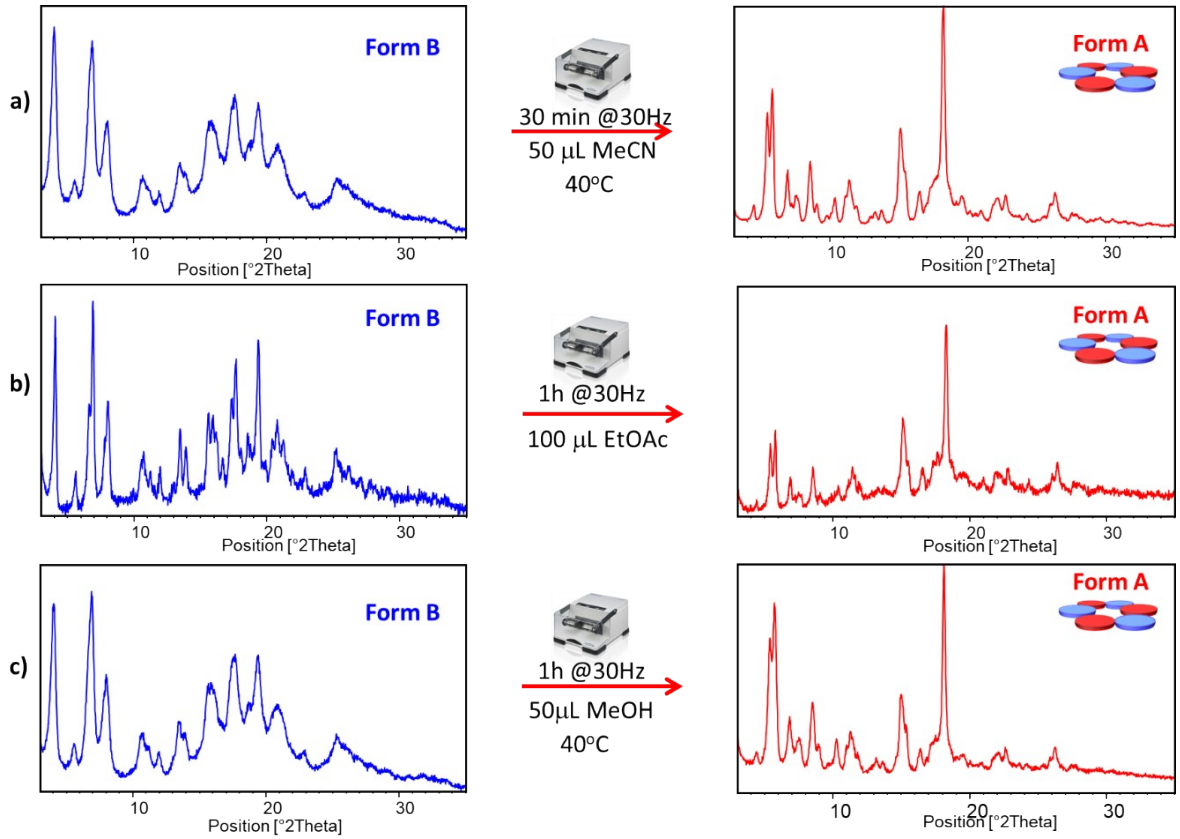

Figure S14. Transformation of **Form B** to **Form A** by LAG with a) MeCN b) ethyl acetate and c) MeOH.

5.4 Milling conditions to transform Form B to the amorphous form

Amorphous form can be obtained from **Form B** on extensive neat grinding which is required to reach a steady-state as shown in Figure S15.

The milling temperature was investigated as part of method development. While milling at 70°C should not change the outcome of the reaction compared to milling at ambient temperature (See 4.1.1), it would significantly improve the rate of the polymorphic transformation.

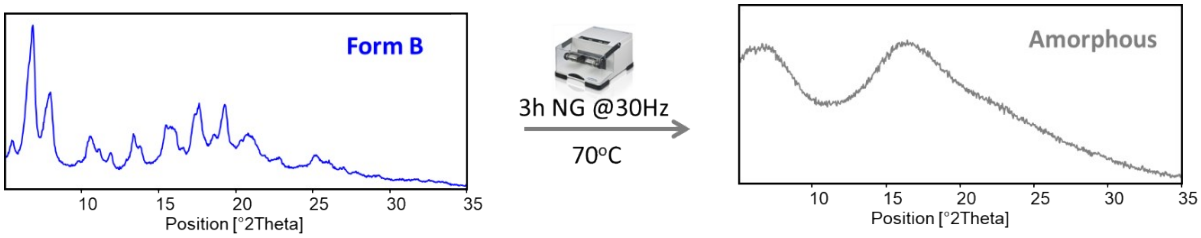

Figure S15. Transformation of **Form B** to the **amorphous form** by ball mill neat grinding over extensive milling time.

5.5 Milling conditions to transform Form A to the amorphous form.

In Section 4.3 we have shown that ball mill neat grinding equimolar amounts of the co-formers (**ME** & **BA**) over an extended time to reach a steady-state, produces predominantly an **amorphous form**.

Similarly, starting from **Form A**, the predominant **amorphous form** is obtained on extensive neat grinding when a steady-state is nearly reached as shown in Figure S16. To obtain the full amorphous form it will be necessary to mill at high temperatures (70°C) to shorten the milling time as observed in Figure S15 (See 4.1.1).

Figure S16. Transformation of **Form A** to the predominant **amorphous form** by ball mill neat grinding over extensive milling time to nearly reach a steady-state.

5.6 Milling conditions to transform the amorphous form to Form A

In Section 4.2 we have shown that ball mill LAG equimolar amounts of the co-formers (**ME** & **BA**) to a steady-state with MeCN, produces **Form A**.

Similarly, starting from the **amorphous form**, **Form A** is obtained by ball mill LAG to a steady-state with MeCN as shown in Figure S17.

Figure S17. Transformation of **amorphous form** to **Form A** by LAG with MeCN.

6 Reversible interconversion between polymorphs of 1:1 ME:BA

All three **1:1 ME:BA** polymorph co-crystals (**Form A**, **Form B** and the **amorphous form**) are reversibly interconverted when milled to a steady-state under the experimental milling conditions favoring the formation of each specific polymorphs as explained in Section 5.

Section 6.1 Reversible polymorph interconversion between **Form A** and **Form B**
Section 6.2 Reversible polymorph interconversion between **Form A** and the **amorphous form**
Section 6.3 Reversible polymorph interconversion between **Form B** and the **amorphous form**

6.1 Reversible polymorph interconversion between Form A and Form B

As shown in figure S18, **Form A** can be interconverted to **Form B** by ball mill LAG to a steady-state with water. Dried **Form B** can be converted back to **Form A** by ball mill LAG to a steady-state with MeOH, though it would have equally worked if MeCN was used instead of MeOH.

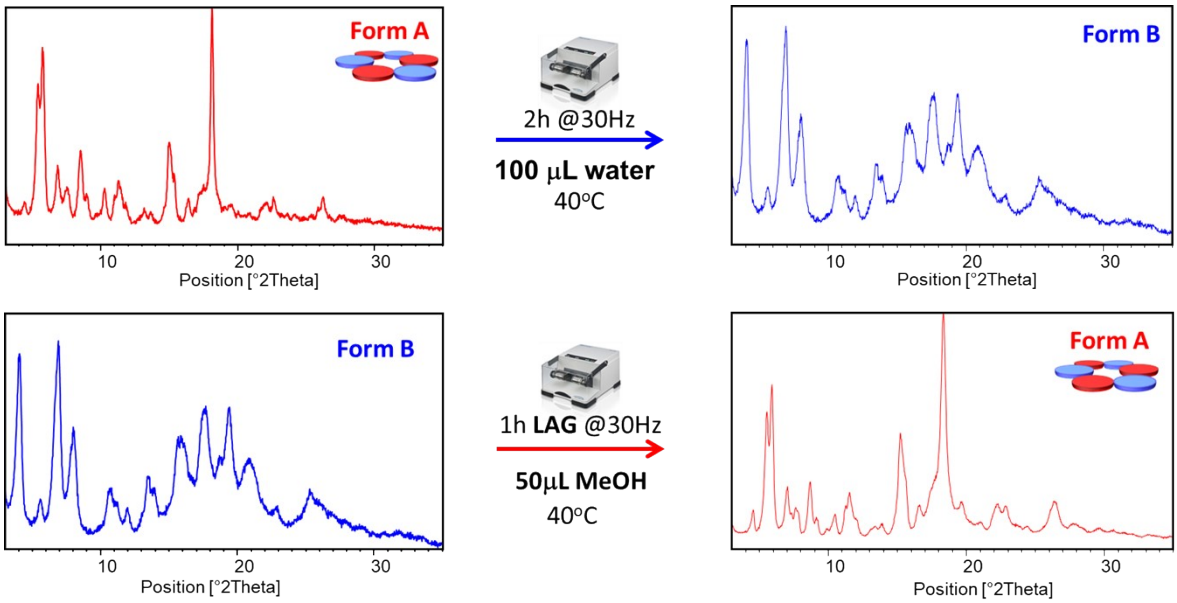

Figure S18. Reversible transformation between **Form A** and **Form B**. a) example of transformation of **Form A** to **Form B** by LAG with water. b) example of transformation of **Form B** to **Form A** by LAG with MeOH as LAG solvent. MeCN or ethyl acetate as shown in Section 5.3 can also be used as LAG solvents to convert **Form B** to **Form A**.

6.2 Reversible polymorph interconversion between Form A and amorphous form

As shown in figure S19, **Form A** can be predominantly converted to the **amorphous form** by ball mill NG to a steady-state. The **predominant amorphous form** can be converted back to **Form A** by ball mill LAG to a steady-state with MeCN.

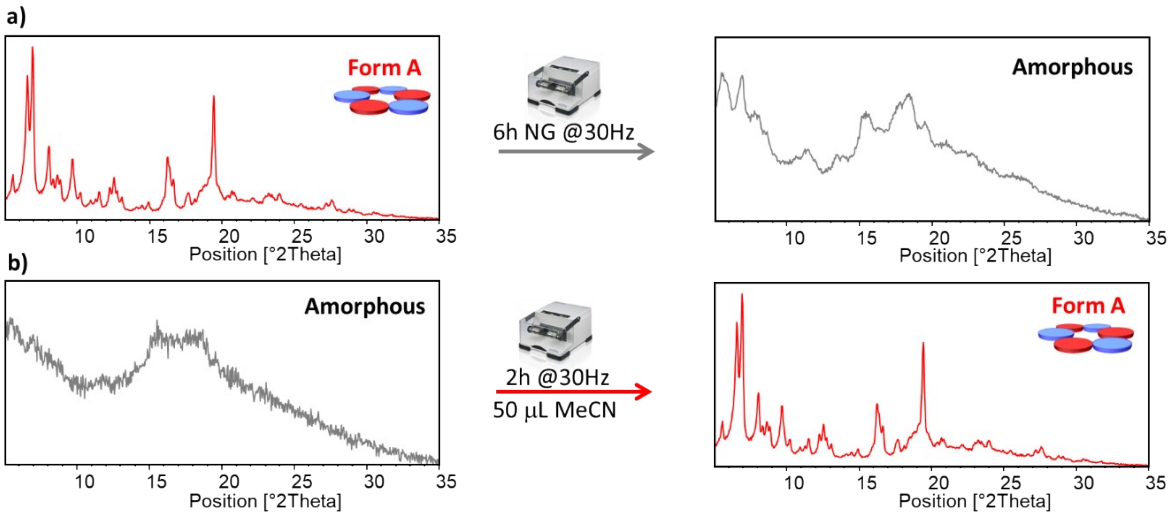

Figure S19. Reversible transformation between the predominant **amorphous form** and **Form A**. a) example of transformation of **Form A** to the predominant **amorphous form** by NG. b) example of transformation of predominant **amorphous form** to **Form A** by LAG with MeCN as LAG solvent.

6.3 Reversible polymorph interconversion between Form B and amorphous form

As shown in figure S20, the predominant **amorphous form** can be converted to **Form B** by ball mill LAG with water to a steady-state. Dried **Form B** can be converted back to the **amorphous form** by ball mill NG to a steady-state. While milling at 70°C should not change the outcome of the reaction compared to milling at ambient temperature, it would significantly increase the rate of the polymorphic transformation (See 4.1.1).

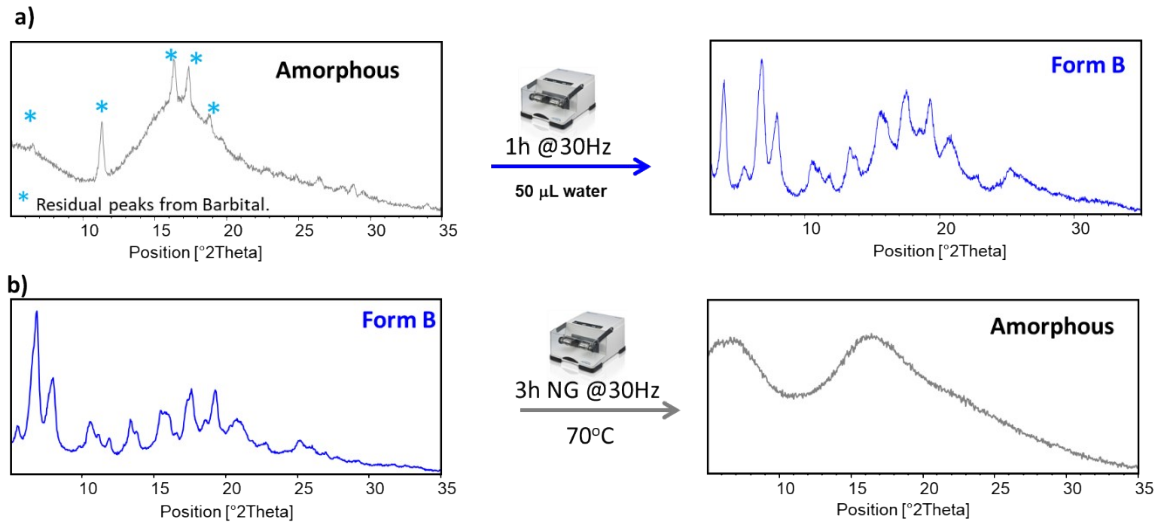

Figure S20. Reversible transformation between **amorphous form** and **Form B**. a) example of transformation of **amorphous form** to **Form B** by LAG with water. b) example of transformation of **Form B** to **amorphous form** by neat grinding to a steady-state.

6.4 Summary of polymorph transformation between Form A, Form B and amorphous form

The scheme below (Figure S21) summarizes the polymorph formation and interconversion discussed in Section 5 and Section 6.1 to 6.3. **Form A** and the **amorphous form** of **1:1 ME:BA** can be obtained starting from the co-formers (**BA** and **ME**) by ball milling to steady-state. **Form B** is obtained by polymorph interconversion from either the **amorphous form** or from **Form A**. All the polymorphs can interconvert to each other by applying milling conditions which favours their formation and grind until steady-state is reached.

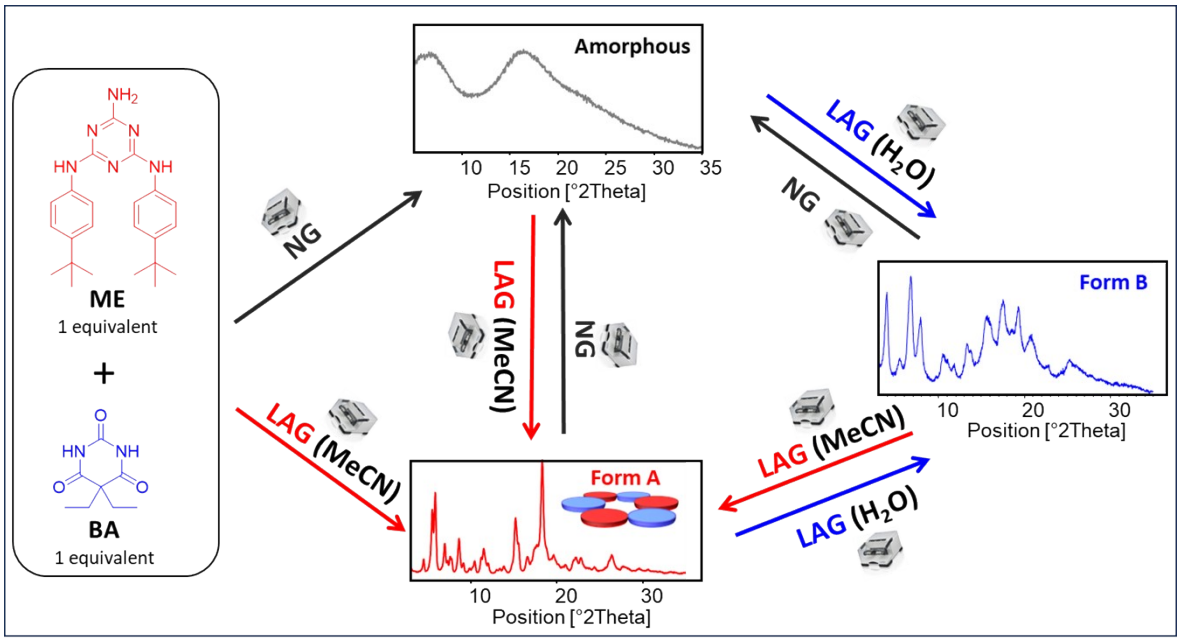

Figure S21. Summary of the formation of the 1:1 **ME:BA** polymorphs at steady-state from the equimolar ratio of the conformers (**ME** & **BA**) forming by NG, the **amorphous form** and by LAG with MeCN, **Form A** (rosette form). **Form B** is obtained by polymorph interconversion by LAG with water starting from the **amorphous form** or from **Form A**. All 3 polymorphs can interconvert by applying the suitable milling conditions and milling to steady-state.

7 Ball milling strategies to improve resolution of the crystallinity of Form B

7.1 Thermal annealing of Form B

After the preparation of **Form B**, the crystals of **Form B** were subjected in an oven to high temperature to anneal them in order to improve their crystallinity as shown in Figure S22. This approach was totally unsuccessful as seen by the poorly resolved PXRD patterns.

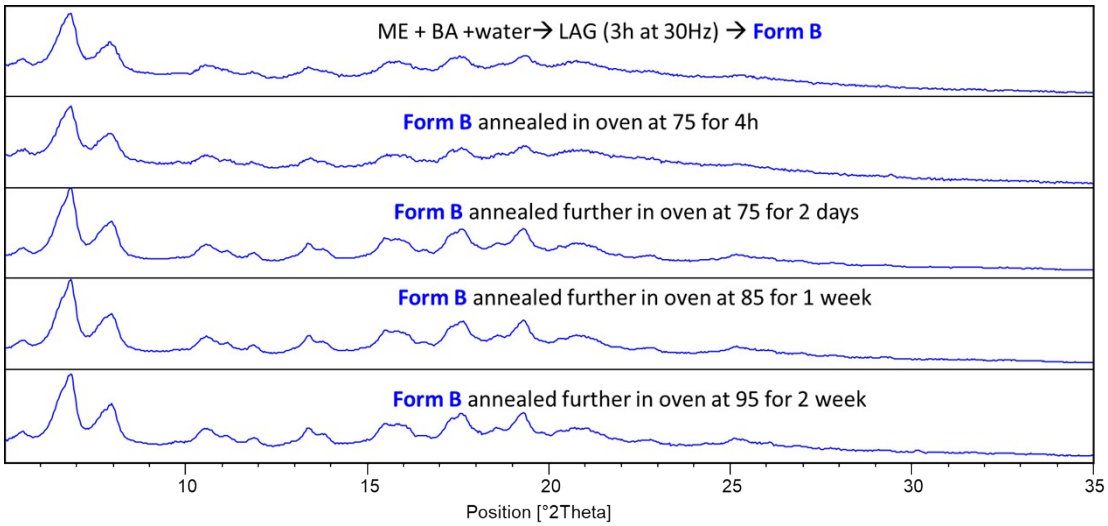

Figure S22. Procedure for annealing **Form B** in an oven. **Form B** was initially obtained from **amorphous form** by ball mill LAG with 50 µL water for 2h at RT at 30 Hz. Crystallinity of **Form B** was not improved by annealing in an oven as can be seen from the broad peaks in the resulting PXRD scans. These PXRD patterns are not suitable to determine the crystal structure of **Form B**.

7.2 Mechanochemical annealing of Form B

In order to determine the crystal structure of **Form B**, we required to obtain a more crystalline material so that the PXRD patterns would have sharper and better resolved peaks. Unfortunately, the improvement by mechanochemical annealing shown in Figure S23 was not suitable for crystal structure determination.

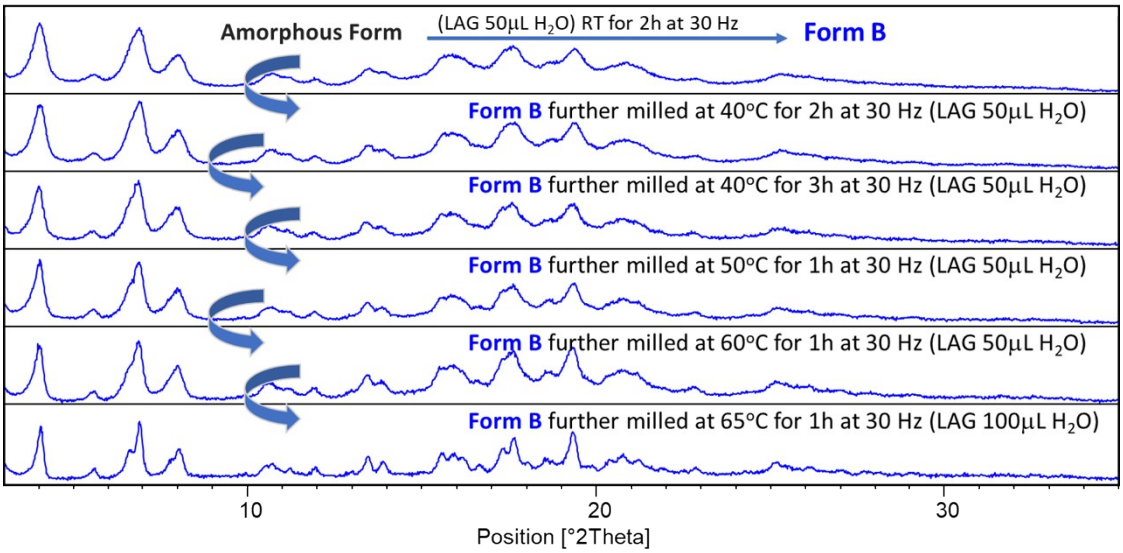

Figure S23. Preparation of more crystalline **Form B** by repeatedly milling at 40˚C up to 65°C with water as a LAG solvent. A slight improvement of crystallinity can be observed after milling at 65°C with 50 µL of water.

8 Disappearance of Form B. Replacement by Form C

We expected to obtain **Form B** when equimolar amounts of **ME** and **BA** were milled under LAG conditions to a steady-state using water as the LAG solvent. We had previously consistently obtained **Form B** from a polymorph interconversion under LAG conditions to a steady-state with water starting either from the **amorphous form** (See Section 4.4.1) or from **Form A** (See Section 4.4.2). Instead, we obtained a new polymorph, which we named **Form C**.

Normally the outcome of ball milling should have been the same regardless of, if we start from the co-formers in the expected ratio (1:1) or from any other polymorph obtained with those co-formers in the same ratio. The formation of **Form C** under the experimental milling conditions to form **Form B** was totally unexpected.

8.1 Mechanochemical synthesis of Form C. Procedure

Form C was obtained by LAG with water from equimolar amounts of the co-formers (**ME** & **BA**) milling at 30Hz to a steady-state. From this moment on, **Form B** could no longer be formed by polymorph interconversion using the same conditions as in Section 4.4. Instead, we consistently obtained **Form C** under LAG conditions with water. **Form B** had disappeared.

Procedure: Equimolar amounts of **ME** (0.35 mmol, 136.7 mg) and **BA** (0.35 mmol, 64.5 mg) were added to a 14.5 mL home-made screw closure jar (Figure S2-a). The crystals of **ME** and **BA** were manually mixed in the jar with a microspatula before milling. Two 7.0 mm 440C stainless steel were added to the jar. 50 µL of water was dispensed on top of the powder. The jar was screw closed and secured with insulating tape. On installing the jar in the MM400 grinder, it was milled under LAG conditions for 3 h at 30 Hz obtaining **Form C** quantitatively at steady-state. (See Figure S24-a)

Similarly, using a narrower 4 mL snap closure 316 stainless steel jar (Figure S2-b&c), **ME** (0.122mmol, 47.7mg) and **BA** (0.122 mmol, 22.5 mg) were added, the powder was mixed with a microspatula and 2x5mm diameter, 315 stainless steel balls were added. 20 µL water was dispensed on top of the powder. The jar was closed, and the junction sealed with insulating tape. On installing the jar in the MM400 grinder, it was milled under LAG conditions for 3 h at 30 Hz obtaining **Form C** quantitatively at steady-state. (See Figure S24b).

Both 200 mg loading (Figure S24a) and 70 mg loading (Figure S24b) produced pure **Form C**.

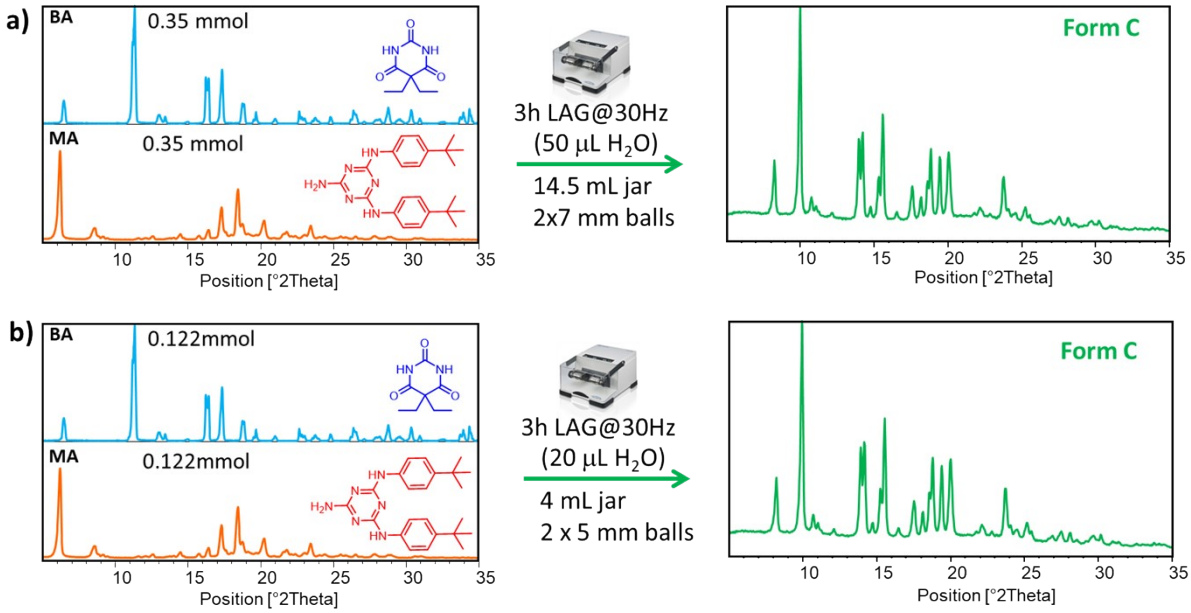

Figure S24. PXRD pattern on the left on a) and b) the 2 co-formers (top left: **BA**) and (bottom left: **MA**). On the right, the 1:1 **ME:BA** co-crystal **Form C** obtained by ball mill LAG using water as the LAG solvent. a) prepared at 200 mg scale; b) prepared at 70 mg scale, both obtaining pure **Form C** at steady-state.

9 Milling conditions required to transform one polymorph to another after the disappearance of Form B

Here we carefully studied the 4 transformations:

Section 9.1: **Form A** to **Form C**

Section 9.2: **amorphous form** to **Form C**

Section 9.3: **Form C** to **Form A**

Section 9.4: **Form C** to **amorphous form**

9.1 Milling conditions to transform Form A to Form C

This transformation was only possible after the disappearance of **Form B** on forming **Form C** for the first time in our laboratory. See Section 8.1 for the formation of **Form C** from milling the equimolar amount of the co-formers (**ME** and **BA**) in the presence of water as LAG solvent. **Form C** is also obtained on milling **Form A** in the presence of water. Previously we would have obtained **Form B** using the same experimental milling conditions. For the implication of milling at higher temperature see 4.1.1.

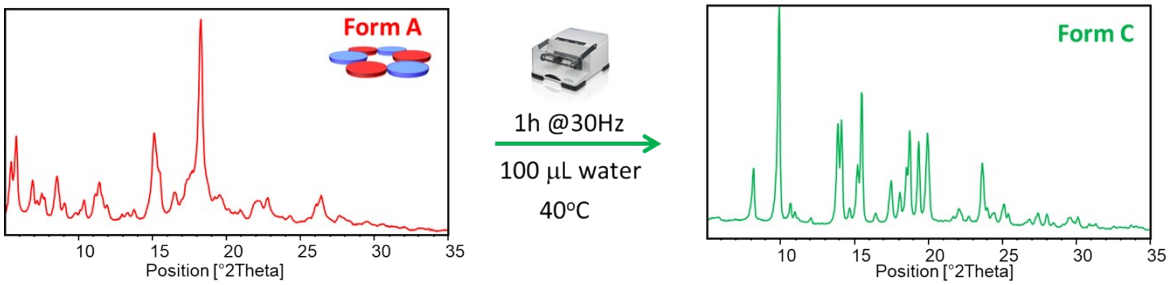

Figure S25. Transformation of **Form A** to **Form C** by LAG with water, after **Form B** has disappeared on first forming **Form C**.

9.2 Milling conditions to transform the amorphous form to Form C

Ball milling under LAG with water to steady-state transforms the **amorphous form** to **Form C** as shown in Figure S26.

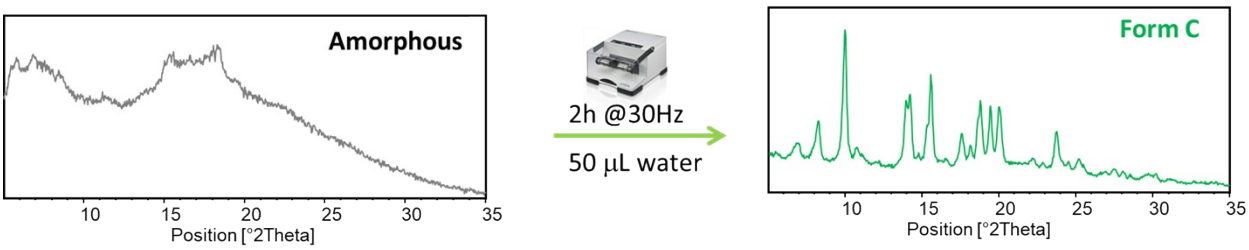

Figure S26. Transformation of **amorphous form** to **Form C** by LAG with water, after **Form B** has disappeared on first forming **Form C**.

9.3 Milling conditions to transform Form C to Form A

Form A was formed by polymorph interconversion starting from **Form C** by LAG with acetonitrile (Figure S27). LAG with MeCN always results in the formation of **Form A** by ball mill LAG, even with only 20 µL of MeCN/200 mg powder.

Figure S27. Transformation of **Form C** to **Form A** by LAG with MeCN.

9.4 Milling conditions to transform Form C to the amorphous form

As in Section 5.4 (starting from **Form B**) and 5.5 (starting from **Form A**), amorphous form can also be obtained from **Form C** on extensive neat grinding as shown in Figure S28.

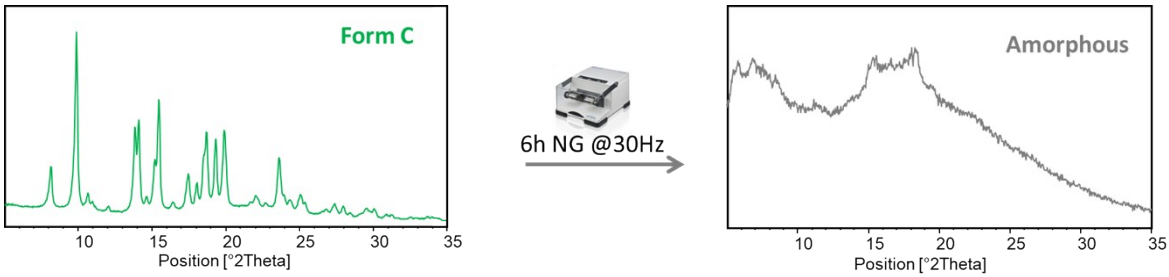

Figure S28. Transformation of **Form C** to predominant **amorphous form** by neat grinding over extensive milling time.

10 Reversible interconversion between polymorphs of 1:1 ME:BA after the disappearance of Form B

All three 1:1 **ME:BA** polymorph co-crystals (**Form A**, **Form C** and **amorphous form**) after the disappearance of **Form B**, are reversibly interconverted when milled to steady-state under the right experimental milling conditions.

Section 10.1 Reversible polymorph interconversion between **Form A** and **Form C**
Section 10.2 Reversible polymorph interconversion between **Form C** and the **amorphous form**
Section 6.2: Reversible polymorph interconversion between **Form A** and the **amorphous form**. (The reversible polymorph interconversion between **Form A** and amorphous form has been already described on Section 6.2).

10.1 Reversible polymorph interconversion between Form A and Form C

As shown in Figure S29, **Form A** can be interconverted to **Form C** by ball mill LAG to a steady-state with water. Dried **Form C** can be converted back to **Form A** by ball mill LAG to a steady-state with MeCN. This polymorph interconversions are only possible after **Form B** had disappeared. For the implication of milling at higher temperature see 4.1.1.

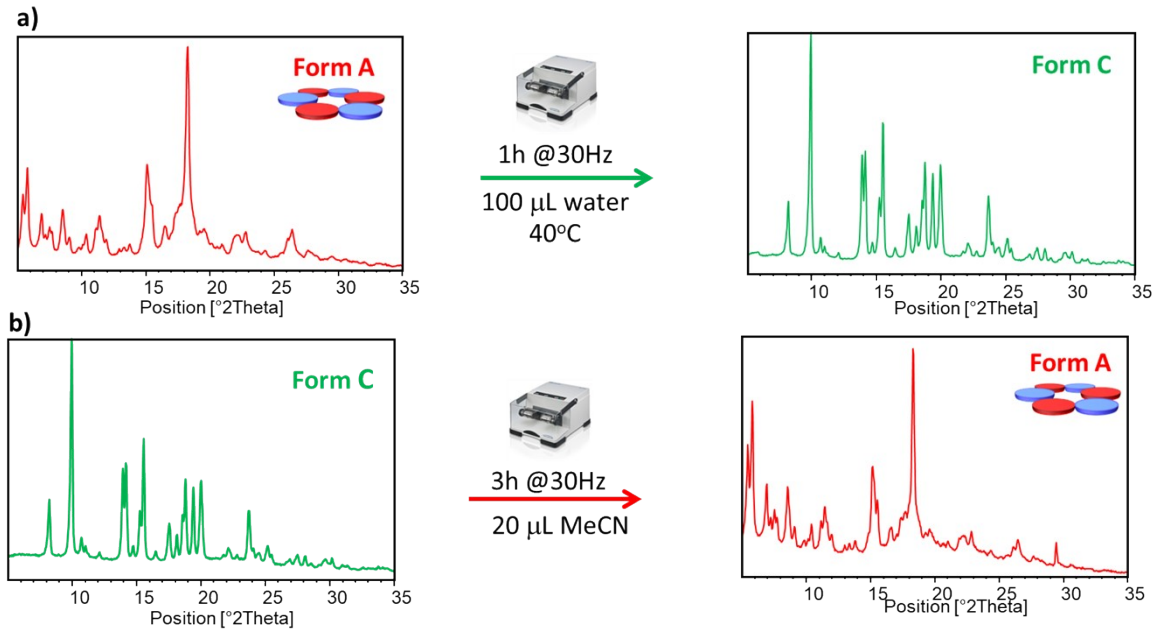

Figure S29. Reversible transformation between **Form A** and **Form C**. Note: this is only possible as **Form B** disappeared once **Form C** was formed. a) example of transformation of **Form A** to **Form C** by LAG with water. b) example of transformation of **Form C** to **Form A** by LAG with MeCN as LAG solvent.

10.2 Reversible polymorph interconversion between Form C and amorphous form

As shown in Figure S30, **Form C** can be converted to the **amorphous form** by ball mill NG to a steady-state. The **amorphous form** can be converted back to **Form C** by ball mill LAG to a steady-state with water. This polymorph interconversions are only possible after **Form B** had disappeared.

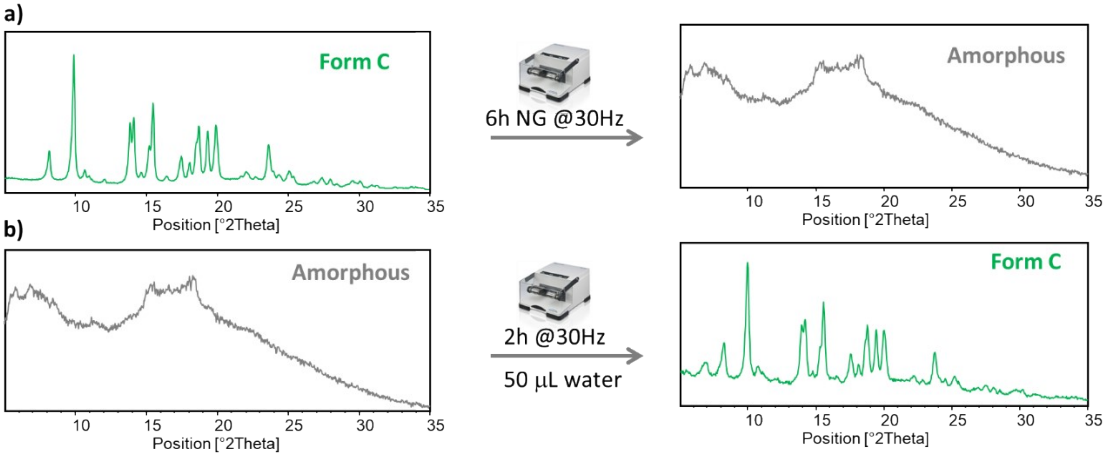

Figure S30. Reversible transformation between **Form C** and **amorphous form**. a) example of transformation of **Form C** to predominant **amorphous form** by extended neat grinding. b) example of transformation of **amorphous form** to **Form C** by LAG with water.

10.3 Summary of polymorph transformation between Form A, Form C and amorphous form

The scheme below (Figure S31) summarizes how the 1:1 **ME:BA Form C** can be obtained from the co-formers (**BA** and **ME**) by ball milling with water to steady-state. After the first appearance of **Form C**, **Form B** disappears. **Form C** is also obtained by polymorph transformation of **Form A** and the **amorphous form** by LAG with water. The **amorphous form** is obtained by polymorph transformation of **Form C** and **Form A** by NG. **Form A** is obtained by polymorph transformation of **Form C** and the **amorphous form** by LAG with MeCN. All the polymorphs can interconvert to each other by applying the right milling conditions and milling to steady-state.

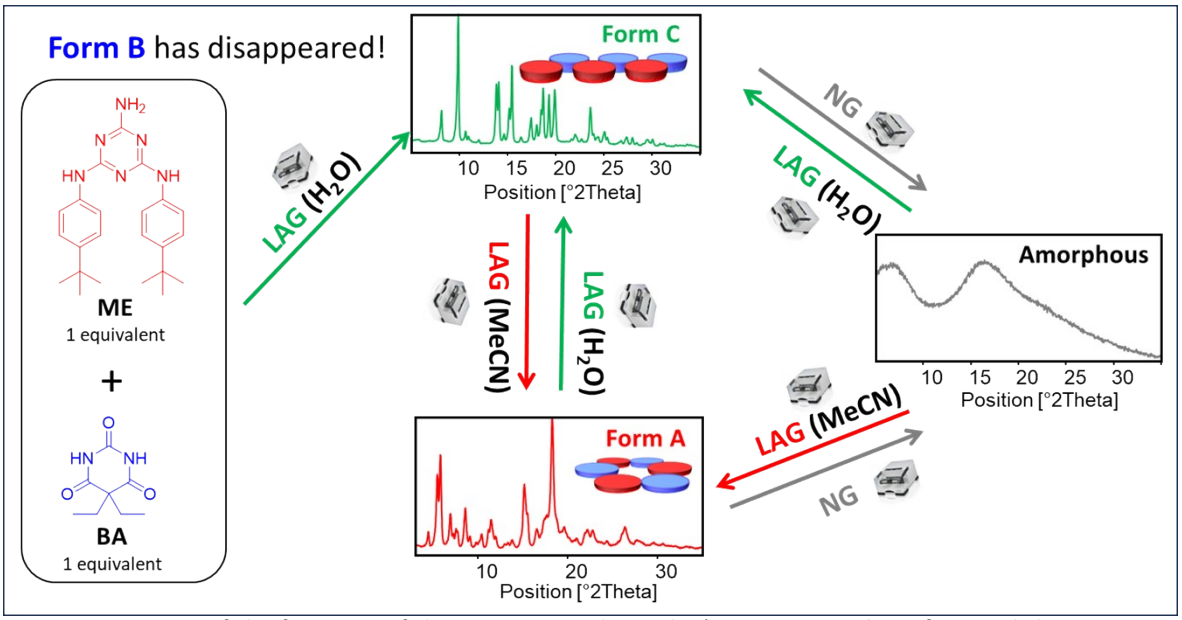

Figure S31. Summary of the formation of the 1:1 **ME:BA** polymorphs (**Form A**, **amorphous form** and the new **Form C**). Preparation of **Form C** from the equimolar ratio of the conformers (**ME** & **BA**) by LAG with water milled to steady-state. **Form C** is also obtained by polymorph transformation of **Form A** or the **amorphous form** by LAG with water. A**morphous form** is obtained by NG from **Form A** or **Form C** when milled to steady-state. **Form A** (rosette form) is obtained from **Form C** and from the **amorphous** form by LAG with MeCN. All 3 polymorphs can interconvert by applying the suitable milling conditions and milling to steady-state.

11 Validation that Form B has disappeared after formation of Form C

11.1 Proof of disappearance of Form B

Form B was originally obtained either from the **amorphous form** by LAG with water as shown in Figure S11 or from **Form A** by LAG with water as shown in Figure S12.

To validate that **Form B** had disappeared in our laboratories after the first appearance of **Form C**, the **amorphous form** (See Figure S30-b) and **Form A** (Figure 29-a) were prepared again.

LAG with water starting from the amorphous form is shown in Figure S32-b, leading to the formation of **Form C**, instead of what was previously formed, which was **Form B** (Figure S32-a).

Figure S32 compares the outcome of milling the amorphous form under LAG with water before (Figure S32-a) and after (Figure S32-b) the first appearance of **Form C**.

a) Preparation of **Form B** by LAG with water from **amorphous** form , as in Figure S11 before **Form C** appeared first time

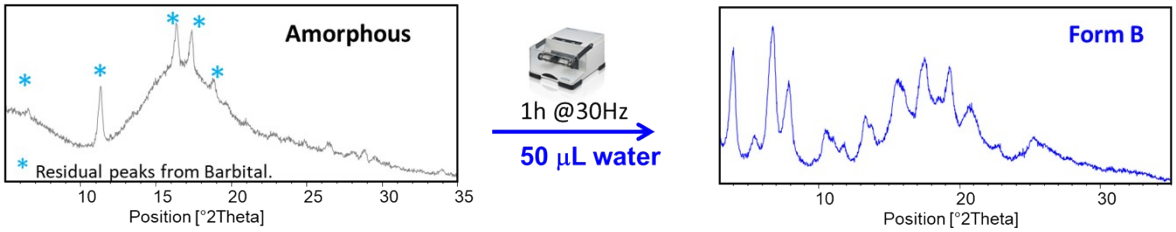

b) **Form B** has disappeared after **Form C** appeared for the first time. LAG with water of **amorphous form** leads now to **Form C** as in Figure S26.

Figure S32. Comparison of the effect of milling the **amorphous form** under LAG conditions with water to steady-state. a) before the first appearance of **Form C** leading to the formation of **Form B**, b) after the first appearance of **Form C**, obtaining only **Form C** instead of the disappeared **Form B**.

Figure S33 compares the outcome of milling **Form A** under LAG with water to steady-state before (Figure S33-a) and after (Figure S33-b) the first appearance of **Form C**. For the implication of milling at higher temperature see 4.1.1.

a) Preparation of **Form B** by LAG with water **from Form A**, as in Figure S12 before **Form C** appeared for the first time.

b) **Form B** has disappeared after **Form C** appeared for the first time. LAG with water of **Form A** leads now to **Form C** as in Figure S25.

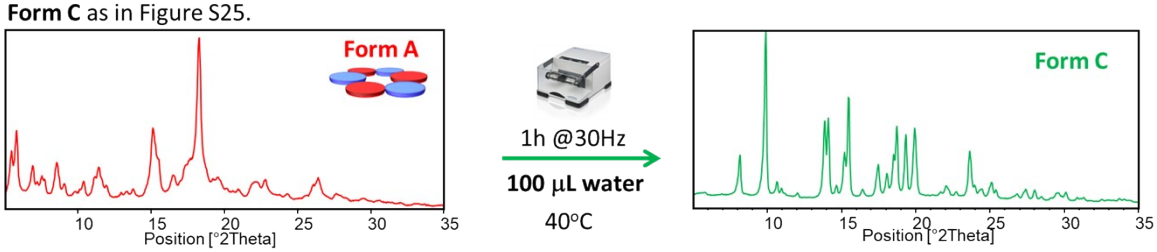

Figure S33. Comparison of the effect of milling **Form A** under LAG conditions with water to steady-state. a) before the first appearance of **Form C** leading to the formation of **Form B**, b) after the first appearance of **Form C**, obtaining only **Form C** instead of the disappeared **Form B**.

In conclusion, **Form B** has disappeared in our laboratory in the Department of Chemistry at the University of Cambridge.

11.2 Mechanochemical annealing procedure of Form C

Form C could only be prepared consistently after **Form B** polymorph had dissapeared. In order to get a good PXRD scan, we needed to obtain a good crystalline **Form C** suitable for crystal structure determination. The PXRD pattern shown in Figure 34-b was used for the crystal structure determination of **Form C.**

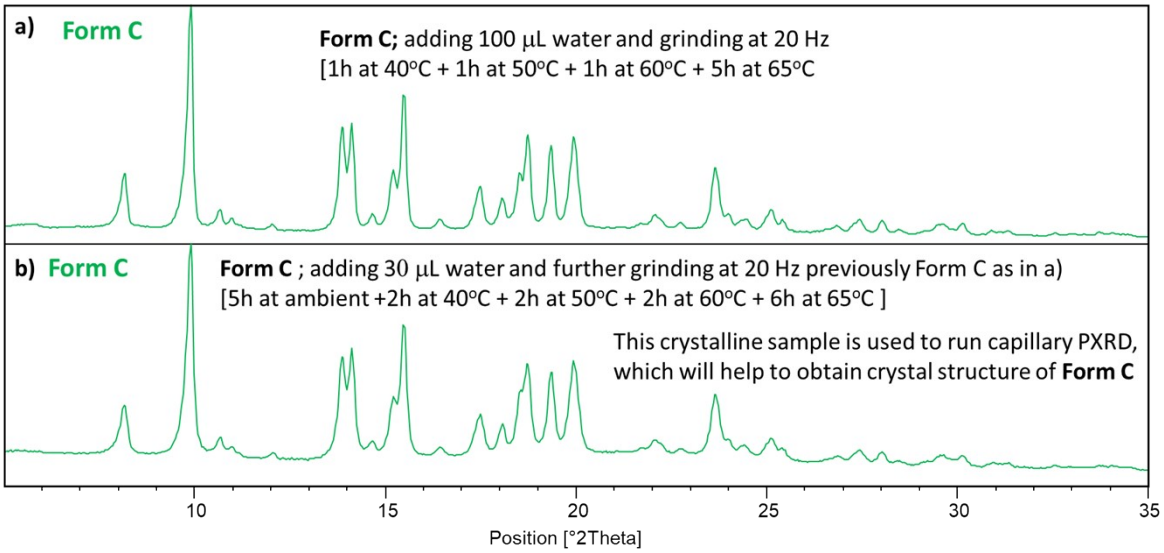

Figure S34. Steps taken to grind **Form C** in the presence of water at ambient to 65°C as described on the PXRD patterns to obtain suitable PXRD for crystal structure determination.

12 Comparison of PXRDs of the 4 polymorphs of 1:1 ME:BA obtained by ball milling

The PXRD patterns of **ME** and **BA** and all 4 polymorphic forms of the 1:1 **ME:BA** are shown in Figure S35.

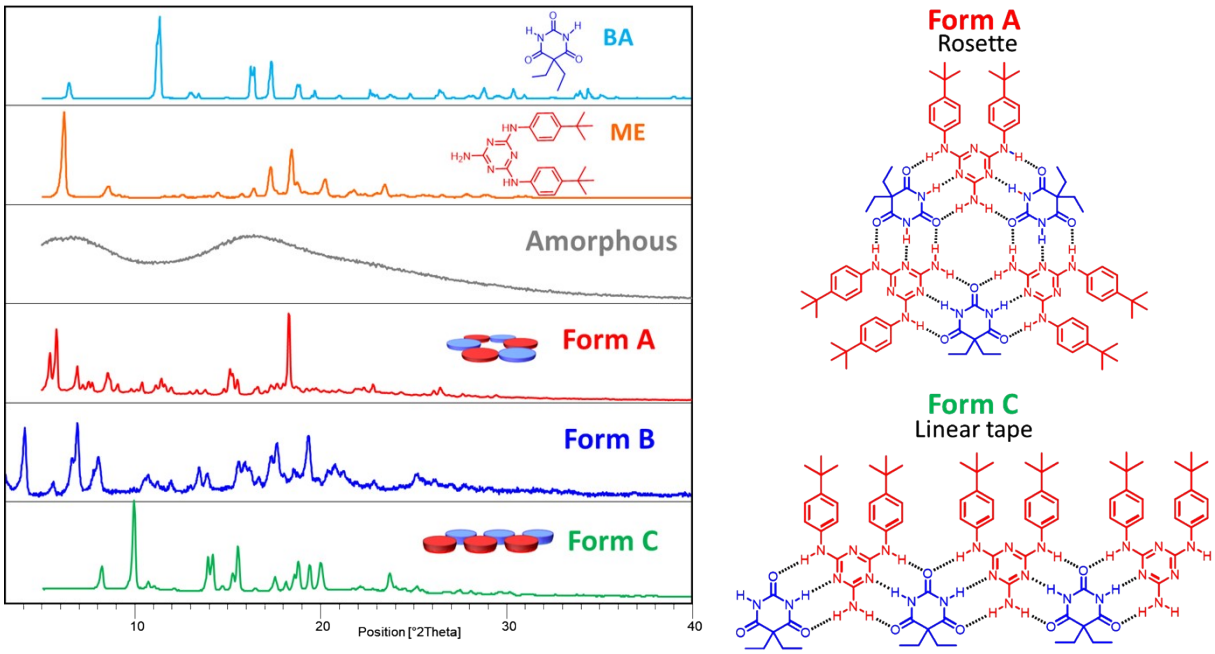

Figure S35. Comparative PXRD patterns of the co-formers and the 4 polymorphs of 1:1 **ME:BA.** **Form A, Form C** and the **amorphous form** were formed by ball milling equimolar amounts of **ME** and **BA.** **Form B** was instead obtained by polymorph conversion from **Form A** or from the **amorphous form** by LAG with water. **Form B** disappeared on first appearing **Form C.**

13 PXRD suitable for structure elucidation of Form C

X-ray powder diffractograms in the 2θ range 4-45° (Cu Kα radiation, λ = 1.54106 Å, step size 0.03°, time/step 100 s, 0.04 rad soller, VxA 40x40) were collected on a Panalytical X'Pert Pro diffractometer equipped with an X'Celerator detector.

The powder pattern of **Form C** (Figure S36) was indexed using DICVOL[12] in DASH,[13] and TOPAS.[14-16] Structure solution was achieved by the real-space method, using simulated annealing routine implemented in DASH.[13] When using the Hofmann's volume increments,[17] the expected molecular volume found was 771.9 Å^3, corresponding to two molecules in the unit cell (Z = 2) for a unit cell volume of 1645.9 Å^3 (Table S1). The starting model of **BA** was obtained from the cif file of CSD (Cambridge Structural Database) with the entry DETBAA03. **ME** model was generated by modifying the structure of the cif file with the CSD entry BEYXUY. During simulated annealing no restrictions in the degrees of freedom were applied.

Rietveld refinement was performed with Topas Academic V7.[14-16] The instrumental parameters were determined with LaB6 NIST standard 660b[18] using a fundamental parameters approach. A shifted Chebyshev function with 12 parameters was used to fit the background. The sample contribution to peak broadening was modelled with two isotropic Lorentzian parameters, one for crystallite size, and one for microstrain. Restraints were applied on all bond distances and all bond angles. Correction for preferred orientation was achieved with an 8th order spherical harmonics model. Refinement converged and the details can be found on table S1. The structure of **Form C** (Figure S37) was deposited on CCDC with the number 2373751.

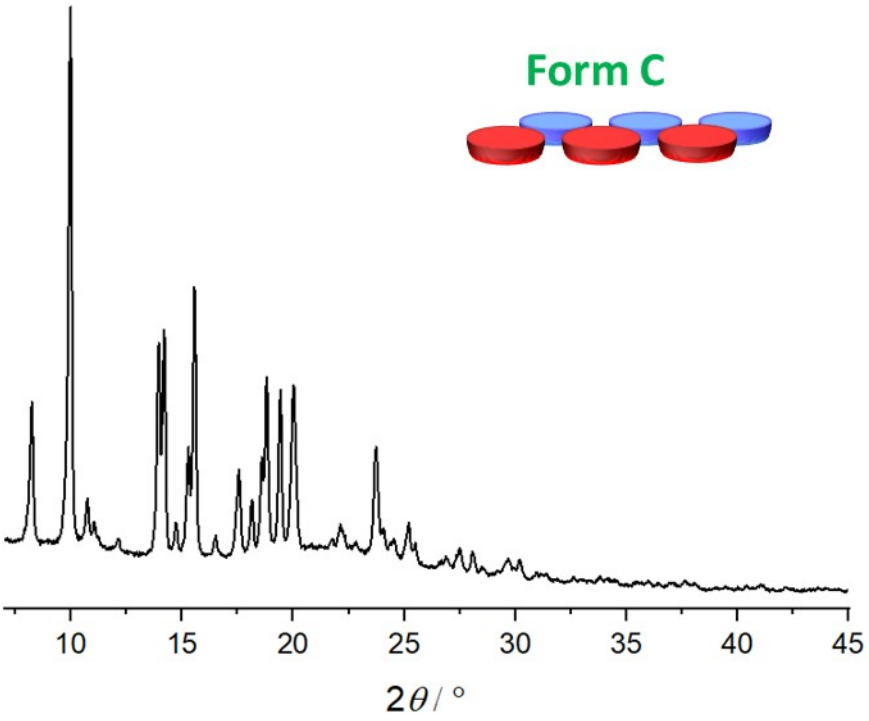

Figure S36. Calculated PXRD of **Form C**.

Table S1 Crystallographic details for **BA·ME Form C.**

	BA·ME (form C)
Chemical formula	$C_{31}H_{42}N_8O_3$
Formula weight/g.mol^{-1}	
Crystal system	Monoclinic
Space group	*P* 2_1
a/Å	9.6921(8)
b/Å	15.7727(14)
c/Å	12.6377(12)
β/°	121.623(6)
V/Å^3	1645.92(2)
Z	2
R_p, R'_p/%[1]	3.5303, 11.0980
R_{wp}, R'_{wp}/%[1]	4.4952, 11.4635
R_{exp}, R'_{exp}/%[1]	1.9767, 5.0410
R_{Bragg}/%	1.6006
GoF (χ^2)	2.2740

*Dashed values correspond to values after background subtraction.

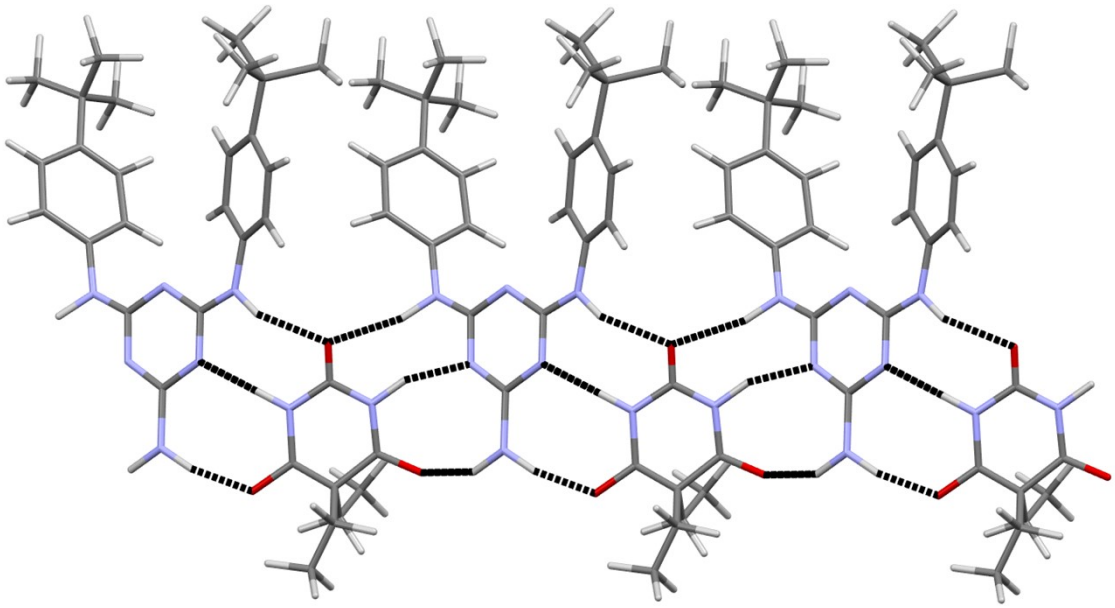

Figure S37 Structure of **Form C.**

14 References

1. J. P. Mathias, E. E. Simanek, C. T. Seto and G. M. Whitesides, *Angewandte Chemie International Edition in English*, 1993, **32**, 1766-1769.
2. A. M. Belenguer, G. I. Lampronti and J. K. M. Sanders, *Israel Journal of Chemistry*, 2021, **61**, 764-773.
3. Ana M. Belenguer, A. A. L. Michalchuk, G. I. Lampronti and J. K. M. Sanders, *Beilstein J. Org. Chem.*, 2019, **15**, 1226–1235.
4. A. M. Belenguer, G. I. Lampronti and J. K. M. Sanders, *JoVE*, 2018, DOI: doi:10.3791/56824, e56824.
5. A. M. Belenguer, G. I. Lampronti, A. J. Cruz-Cabeza, C. A. Hunter and J. K. M. Sanders, *Chem. Sci.*, 2016, **7**, 6617-6627.
6. A. M. Belenguer, G. I. Lampronti, D. J. Wales and J. K. M. Sanders, *Journal of the American Chemical Society*, 2014, **136**, 16156-16166.
7. A. M. Belenguer, T. Friscic, G. M. Day and J. K. M. Sanders, *Chem. Sci.*, 2011, **2**, 696-700.
8. A. M. Belenguer, G. I. Lampronti, N. De Mitri, M. Driver, C. A. Hunter and J. K. M. Sanders, *Journal of the American Chemical Society*, 2018, **140**, 17051-17059.
9. J.-F. Willart, J. Lefebvre, F. Danède, S. Comini, P. Looten and M. Descamps, *Solid State Communications*, 2005, **135**, 519-524.
10. J. Alić, I. Lončarić, M. Etter, M. Rubčić, Z. Štefanić, M. Šekutor, K. Užarević and T. Stolar, *Physical Chemistry Chemical Physics*, 2024, **26**, 4840-4844.
11. K. Linberg, P. C. Sander, F. Emmerling and A. A. L. Michalchuk, *RSC Mechanochemistry*, 2024, **1**, 43-49.
12. A. Boultif and D. Louër, *Journal of Applied Crystallography*, 1991, **24**, 987-993.
13. K. Shankland, E. Pidcock, J. Van De Streek, W. I. F. David, W. D. S. Motherwell and J. C. Cole, *Journal of Applied Crystallography*, 2006, **39**, 910-915.
14. H. M. Rietveld, *Acta Crystallographica*, 1967, **22**, 151-152.
15. H. M. Rietveld, *Journal of Applied Crystallography*, 1969, **2**, 65-71.
16. A. Coelho, *Journal of Applied Crystallography*, 2018, **51**, 210-218.
17. D. W. M. Hofmann, *Acta Crystallographica Section B*, 2002, **58**, 489-493.
18. D. R. Black, D. Windover, A. Henins, J. Filliben and J. P. Cline, *Powder Diffraction*, 2011, **26**, 155-158.